

# MicroRNA-92a-3p Regulates Retinal Angiogenesis by Targeting SGK3 in Vascular Endothelial Cells

Yamei Cui, Ruyuan Liu, Yiwen Hong, Yishen Wang, Yanjie Zhu, Tao Wen, Jing Lu, Shudi Mao, Xiao Wang, Jianying Pan, and Yan Luo

State Key Laboratory of Ophthalmology, Image Reading Center, Zhongshan Ophthalmic Center, Sun Yat-sen University, Guangzhou, Guangdong, China

Correspondence: Yan Luo, State Key Laboratory of Ophthalmology, Image Reading center, Zhongshan Ophthalmic Center, Sun Yat-sen University, Guangzhou, Guangdong 510060, China; [luoyan2@mail.sysu.edu.cn](mailto:luoyan2@mail.sysu.edu.cn).

YC and RL contributed equally to this work.

**Received:** April 1, 2022

**Accepted:** September 22, 2022

**Published:** October 21, 2022

Citation: Cui Y, Liu R, Hong Y, et al. MicroRNA-92a-3p regulates retinal angiogenesis by targeting SGK3 in vascular endothelial cells. *Invest Ophthalmol Vis Sci.* 2022;63(11):19. <https://doi.org/10.1167/iovs.63.11.19>

**PURPOSE.** The purpose of this study was to investigate the effects and mechanism of microRNA (miR)-92a-3p in retinal angiogenesis in vitro and in vivo.

**METHODS.** The expression of miR-92a-3p was verified by real-time quantitative polymerase chain reaction (RT-qPCR). Agomir-92a-3p was intravitreally injected into the right eye on postnatal day 3 (P3), P5, and P8 in the mice, with the agomir-NC injected left eye as the control. At P7, P9, and P12, immunofluorescence was performed to examine the retinal superficial vascular plexus, deep vascular plexus, proliferation, and apoptosis in retinal vascular endothelial cells (ECs). Human retinal microvascular endothelial cells (HRMECs) were treated with mimic-NC and mimic-92a-3p, then the tube formation, cell migration, and wound healing assays were used to detect the effect of miR-92a-3p on retinal angiogenesis in vitro. Agomir-92a-3p was also intravitreally injected into the right eye of oxygen-induced retinopathy (OIR) mice at P12, with the agomir-NC injected left eye as the control, the neovascularization was observed by retinal flatmount staining with isolectin B4 at P17. Bioinformatics and high-throughput sequencing were performed to identify potential target genes of miR-92a-3p. RT-qPCR and Western blot were carried out to detect the expression of SGK3, p-GSK3 $\beta$ , GSK3 $\beta$ , Bcl-xL, and cleaved caspase-3 in the HRMECs and mouse retinas.

**RESULTS.** The overexpression of miR-92a-3p inhibited the development of retinal superficial vascular plexus and deep vascular plexus, decreased the expression of Ki67, and increased the expression of cleaved caspase-3 in isolectin B4-labeled retinal vascular ECs. In vitro, the overexpression of miR-92a-3p markedly suppressed the tube formation, cell migration, and wound healing of cultured ECs. Overexpression of miR-92a-3p inhibited both in vivo and in vitro physiological angiogenesis by downregulating the expression of SGK3, p-GSK3 $\beta$ /GSK3 $\beta$ , and Bcl-xL. In addition, agomir-92a-3p inhibited the pathological retinal neovascularization of OIR mice, by targeting SGK3, p-GSK3 $\beta$ /GSK3 $\beta$ , and Bcl-xL.

**CONCLUSIONS.** The miR-92a-3p could affect retinal angiogenesis by targeting SGK3 pathway, suggesting that miR-92a-3p may be a potential anti-angiogenic factor for retinal vascular disease.

**Keywords:** miR-92a-3p, retina angiogenesis, endothelial cells, SGK3, oxygen-induced retinopathy (OIR)

Retinal neovascularization contributes to visual loss in several ocular diseases, such as retinopathy of prematurity (184,700 patients at 2010),<sup>1</sup> retinal vein occlusion (28.06 million patients at 2015),<sup>2</sup> and proliferative diabetic retinopathy (150.49 million patients at 2020).<sup>3</sup> Frequent intravitreal injection of anti-vascular endothelial growth factor (VEGF) drugs is the main treatment for retinal neovascularization which causes a big burden for patients and their family. Additionally, about 30% to 40% of the patients experience incomplete response.<sup>4,5</sup> Therefore, understanding the mechanism of retinal angiogenesis and finding novel targets to inhibit retinal angiogenesis is important for the treatment of these ocular vascular diseases.

As stable small ncRNAs, microRNAs (miRNAs) bind to the specific mRNA, then inhibit the transcription or translation

process, and then regulate gene expression. Previous studies have demonstrated that miRNAs may regulate about one-third of human genes,<sup>6</sup> which are related to cell growth, cell proliferation, embryonic development, tissue formation, and various diseases.<sup>7,8</sup> Moreover, miRNAs are also expressed in vascular endothelial cells (ECs), indicating their pivotal role in vascular development.

Our previous study has revealed a spatial-temporal miRNA expression profile<sup>9</sup> and some key miRNAs related to the development of retinal vessels and neurons in postnatal mice. Of these, miR-92a-3p consistently decreases during the retinal development of normal mice. Several miRNAs have been revealed to play an indispensable role in vascular endothelial function and vascular development,<sup>10</sup> and miR-92a is most closely correlated with these courses.<sup>11</sup> It has

been reported that overexpression of miR-92a-3p inhibits the sprouting ability of vascular ECs and the formation of lumen in vitro.<sup>12,13</sup> The role of miR-92a-3p in angiogenesis is still controversial in the existing literature. Some papers<sup>11,13-15</sup> indicate that overexpression of miR-92a in ECs blocks angiogenesis in vitro and in vivo, whereas others<sup>15-18</sup> suggest a pro-angiogenic role for miR-92a-3p.

However, the exact role of miR-92a-3p in regulating retinal angiogenesis remains unclear. Therefore, this study aimed to investigate the effects and mechanism of miR-92a-3p in retinal angiogenesis in vitro and in vivo, and provide a potential therapeutic target for the future treatment of retinal neovascularization diseases.

## MATERIALS AND METHODS

### Animals and OIR Model

All animal experiments were performed strictly following the ARVO Statement for the Use of Animals in Ophthalmic and Vision Research and approved by the Animal Care and Use Committee of Sun Yat-Sen University (permission no. 2020-010). C57BL/6J mice were obtained from Southern Medical University (Guangzhou, China) and raised in a specific pathogen-free room in the laboratory animal center of Zhong Shan Ophthalmic Center (Guangzhou, China). We used a previously described method to produce the OIR model.<sup>50</sup> Details of OIR models were provided in Supplementary Figure S5. The mouse pups normally developed with similar weight were used in our study. The retinas of mice at P7, P9, P12, and P17 were collected for the following experiments.

### Intravitreal Injection

To investigate the effect of miR-92a-3p on retinal vasculature development in postnatal mice, intravitreal injections were performed following previously established procedures.<sup>51,52</sup> Agomirs are specially chemically modified miRNA agonist that functions by mimicking endogenous miRNAs into the miRNA induced silencing complex to regulate the expression of target gene mRNA. Compared with the common miRNA mimics used in cultured cell experiments, agomirs have higher stability and affinity in animals, and are more easily enriched in target cells through cell membrane and tissue gap.<sup>53</sup> Agomir-92a-3p (RiboBio, Guangzhou, China) at a dose of 1  $\mu$ L (1  $\mu$ mol/mL) was intravitreally injected into the right eyes at P3, P5, and P8 using a 10- $\mu$ L Hamilton syringe with a 34-gauge needle. The left eye was intravitreally injected with agomir-NC (RiboBio). At P7, P9, and P12, the retinas were collected to be performed in the study of superficial and deep retinal vasculature layers. In the OIR mouse model, agomir-92a-3p or agomir-NC at a dose of 1  $\mu$ L (1  $\mu$ mol/mL) was intravitreally injected into the right eye at P12, and the retinas were collected at P17 for the study of neovascularization.

### Fluorescein Staining of Retinal Flatmount

To evaluate retinal angiogenesis, a retinal flatmount was used as previously described.<sup>54</sup> Briefly, the dissected whole-mount retinas at P7 or P17 were permeabilized with 0.5% Triton X-100 for 10 minutes, blocked with 20% (v/v) fetal bovine serum (FBS; Gibco, USA) for 1 hour at room temperature, and then stained with vascular marker Alexa568-

conjugated Isolectin B4 (IB4; Invitrogen, USA), together with rabbit anti-Ki67 antibody (CST, USA) or rabbit anti-cleaved caspase-3 antibody (CST, USA). Retinal flatmount images were examined by fluorescence microscope (Olympus, Japan). Adobe Photoshop and ImageJ software were used to analyze retinal angiogenesis (Supplementary Materials and Methods).

### Frozen Section and Immunofluorescence Staining of Retina

For retinal cryosections, the dissected mouse eyes at P9 and P12 were fixed and embedded in optimal cutting temperature compound (Sakura Finetek) at  $-80^{\circ}\text{C}$ , and then sectioned as previously described.<sup>51</sup> Retinal cryosections were stained with Alexa568-conjugated IB4 overnight at  $4^{\circ}\text{C}$ . The retinal sections were washed in phosphate buffer saline (PBS) and incubated with 4',6-diamidino-2-phenylindole (DAPI; Invitrogen, USA) for 5 minutes to visualize cell nuclei. Sections were viewed by fluorescence microscope (Olympus, Japan). ImageJ software was used to analyze retinal vessel formation.

### Cell Culture and Transfection Assays

HRMECs were purchased from Procell Life Science & Technology (Wuhan, China), which were authenticated by short tandem repeat profiling and cultured in a DMEM/F-12 basic medium (Gibco, USA) with 10% FBS (Gibco, USA). HRMECs were transfected with 50 nM mimic-92a-3p or mimic-NC (RiboBio, Guangzhou, China) using a riboFECT™ CP Transfection Kit (RiboBio), according to the manufacturer's instructions. Briefly, HRMECs were transfected 24 hours after being plated in 6-well plates (Corning, NY, USA) with a mixture of synthetic miRNA oligomers and transfection reagent, and added to cells in penicillin-streptomycin-free medium. Cells were then used for endothelial functional assays (tube formation, transwell assay, and wound healing) after 48 hours of transfection. Detailed functional assays are available in Supplementary Materials and Methods.

### Real-Time qPCR

Total RNA was extracted using a Universal microRNA Purification Kit (EZBioscience, USA), according to the manufacturer's instructions. Synthesis of cDNA and RT-qPCR were performed using established protocols, as detailed in the Supplementary Materials and Methods.

### Analysis of Target Genes of MiR-92a-3p

Bioinformatics analysis and high-throughput sequencing were used to identify miR-92a-3p potential target genes. The target genes of miR-92a-3p were predicted with Targetscan and miRDB; DAVID and MetaScape were used to identify the key genes of miR-92a-3p regulating angiogenesis. The extended methodological details are in Supplementary Materials and Methods. High-throughput sequencing and data were analyzed by BGI (Shenzhen, China). Duplicates were used for each group. Gene expression levels were assessed using Bowtie<sup>2</sup><sup>55</sup> and RSEM.<sup>56</sup> Differentially expressed genes (DEGs) were detected using DEGseq algorithm<sup>57</sup>

and filtered by log<sub>2</sub> fold change  $\geq 2.00$  and adjusted *P* value  $\leq 0.001$ .

### Western Blot

Proteins of HRMECs and retinas were extracted by RIPA buffer (Beyotime, Shanghai, China) with protease (Absin, Shanghai, China) and phosphatase inhibitors (Absin, Shanghai, China), according to the manufacturer's instructions. Western blotting was carried out with SurePAGE, Bis-Tris (GenScript, Nanjing, China). Primary antibodies were as follows: rabbit anti-GAPDH antibody (CST, USA), mouse anti-SGK3 antibody (Santa Cruz, USA), rabbit anti-GSK-3 $\beta$  antibody (CST, USA), rabbit anti-Phospho-GSK-3 $\beta$  antibody (CST, USA), rabbit anti-Bcl-xL antibody (CST, USA), and rabbit anti-cleaved caspase-3 antibody (CST, USA). Additional experimental procedures are available in the Supplementary Materials and Methods.

### Statistical Analysis

All data were analyzed and plotted using GraphPad Prism software and presented as the mean  $\pm$  SEM. Statistical differences were analyzed by *t*-test or 1-way ANOVA for multiple comparisons of mean values. Any *P* < 0.05 was considered statistically significant.

## RESULTS

### MiR-92a-3p Gradually Decreases During Mouse Retinal Development

To obtain a detailed spatial-temporal expression profile of miR-92a-3p in the postnatal mouse retina, total RNAs isolated from mouse pup retinas at postnatal days (P)0, P1, P2, P3, P4, P5, P7, P8, P10, P12, P14, and P17 were analyzed for miR-92a-3p expression using real-time quantitative polymerase chain reaction (RT-qPCR). The results showed that the expression of miR-92a-3p was higher during the development stage of superficial retinal vascular (P0–P7) than in the development stage of deep retinal vascular (P8–P17), the course related to a high trend in angiogenic activity. The overall expression was gradually decreasing (Fig. 1A), which

was consistent with the microarray result of our previous study.<sup>9</sup>

### MiR-92a-3p Suppresses the Development of Retinal Vessels

To evaluate the role of miR-92a-3p in developing retinal vessels, we performed intravitreal injection of agomir-92a-3p or agomir-negative control (NC) into the right eyes or left mouse eyes at P3, respectively, when the mouse retinas were mostly devoid of blood vessels. Retinas in both groups were collected 2 days, 3 days, 4 days, and 5 days after intravitreal injection, which correspond to P5, P6, P7, and P8. The expression of miR-92a-3p in the agomir-92a-3p group gradually decreased with time from P5 (*P* = 0.0011 to <0.01) to P8 (*P* < 0.0001), but was still significantly higher than the agomir-NC group (Fig. 1B). To observe the superficial vascular development, retinal flatmounts were analyzed with staining IB4 at P7 mice. The quantification of superficial vascular coverage (Figs. 2A, 2D; *P* = 0.0271 to <0.05), the length of vascular development (Figs. 2A, 2E; *P* = 0.0079 to <0.01), the number of vascular branch points in the proximal retina part (Figs. 2B, 2F, *P* = 0.0135 to <0.05), and the number of endothelial tip cells at the sprouting vascular front (Figs. 2C, 2G; *P* = 0.0152 to 0.05) showed significant decreases in the retinas treated with agomir-92a-3p compared with the agomir-NC group and the normal control group. These results illustrated that the overexpression of miR-92a-3p inhibited the development of mouse superficial retinal vessels.

In addition, agomir-92a-3p or agomir-NC were also intravitreally injected into P5 or P8 mouse eyes, when the superficial vascular plexus partially develop. Retinal frozen sections were analyzed at P9 or P12. Compared to the mice in the other groups, mice in the agomir-92a-3p group had fewer intraretinal vessels diving from the superficial retinal vessels in the posterior retina at P9 (Figs. 3A, 3C; *P* = 0.0084 to <0.01) and fewer peripheral vessels sprouting at P12 (Figs. 3B, 3D; *P* = 0.0002 to <0.001). However, the deep layer vessels had not yet reached the peripheral retina at P9. The deep vascular plexus in the posterior retina at P12 showed no significant difference between the agomir-92a-3p group and the other two groups (Supplementary Figs. S1A, S1B).

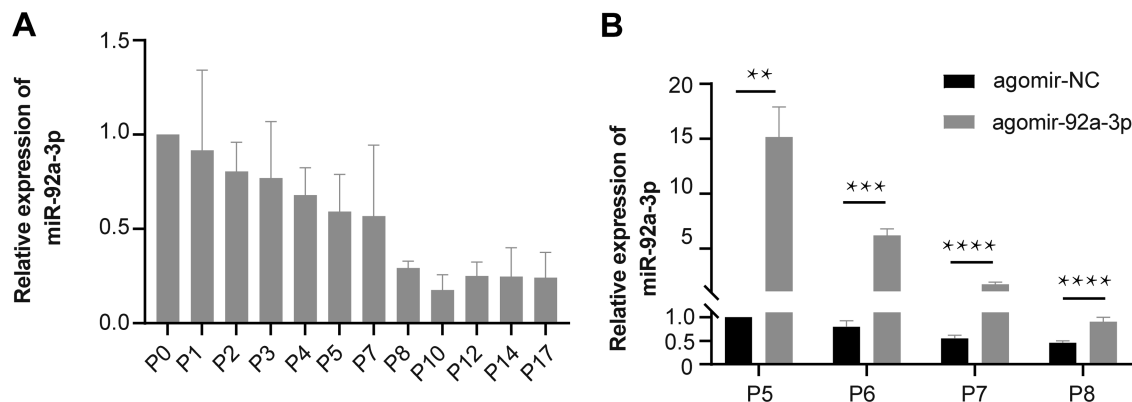


**FIGURE 1.** Expression levels of miR-92a-3p in the mouse retina. **(A)** MiR-92a-3p expression during mouse retinal development: The RT-qPCR showed that miR-92a-3p gradually decreased during the mouse retinal development. **(B)** Changes of miR-92a-3p after the intravitreal injection. The miR-92a-3p expression in mouse retinas of the agomir-92a-3p group declined gradually over time after the intravitreal injection, but was still significantly higher than that of the agomir-NC group (NC = negative control). The data are presented as mean  $\pm$  SD (*n* = approximately 3–6 per group). \*\**P* < 0.01, \*\*\**P* < 0.01, \*\*\*\**P* < 0.0001.

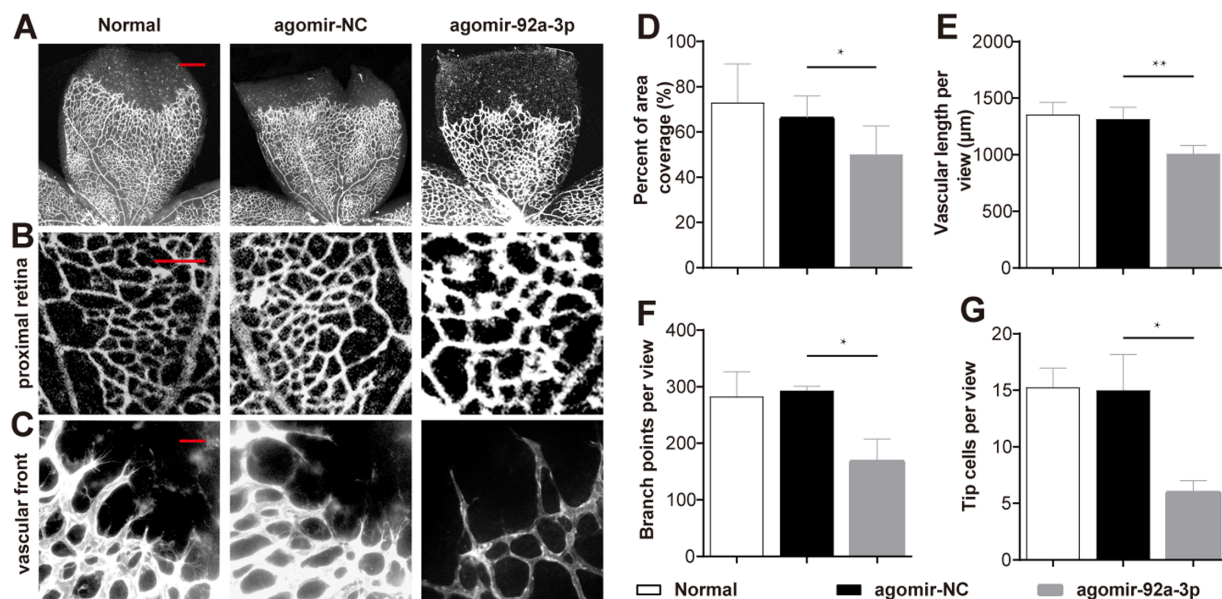


**FIGURE 2.** MiR-92a-3p inhibits the development of superficial retinal vessels. (A–C) Representative images of P7 mouse retinas injected with agomir-92a-3p or agomir-NC at P3, respectively, followed by staining with vascular marker IB4 to observe the superficial retinal vessels. Scale bar, A (500 μm), B (200 μm), and C (50 μm). (D) Quantification of the superficial vascular coverage. (E) Length of vascular development. (F) Number of vascular branch points in the proximal retina. (G) Significant decrease in the number of endothelial tip cells at the sprouting vascular front of the retinas treated with agomir-92a-3p compared to the agomir-NC and normal groups. The data are presented as mean ± SD ( $n =$  approximately 3–6 per group). \* $P < 0.05$ , \*\* $P < 0.01$ .

These data suggested that agomir-92a-3p affected the development of the deep retinal vascular plexus.

### MiR-92a-3p Alters Proliferation and Apoptosis of Retinal Vascular ECs

Previous literature has suggested that vascular ECs can be localized using IB4.<sup>19</sup> To further address the role of miR-92a-3p in retinal angiogenesis, we used a retinal whole mount stained with the proliferation marker Ki67, the apoptosis marker cleaved caspase-3, and the ECs marker IB4. Retinas treated with agomir-92a-3p exhibited fewer Ki67 positive ECs at the vascular front ( $P < 0.05$ ; Figs. 4A, 4C;  $P = 0.0091$  to  $< 0.01$ ). By contrast, the agomir-92a-3p group revealed a significant increase in the proximal retina stained with cleaved caspase-3 compared with the agomir-NC and normal groups (Figs. 4B, 4D;  $P = 0.0217$  to  $< 0.05$ ). Together, these results indicate that agomir-92a-3p inhibits the proliferation and promotes the apoptosis of vascular ECs in the middle retina and eventually the peripheral retina.

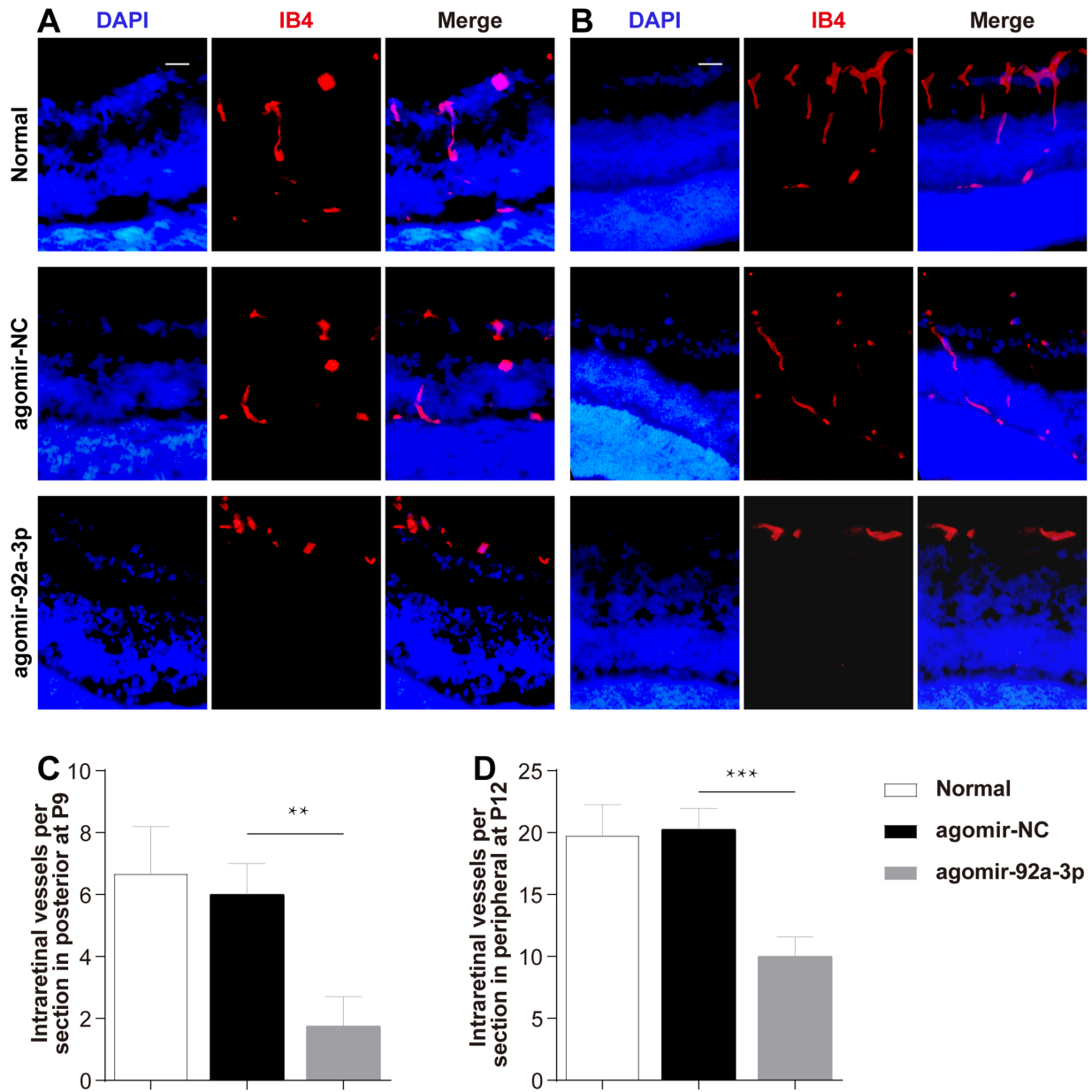
### MiR-92a-3p Suppresses the Tube Formation, Migration, and Proliferation of Human Retinal Microvascular Endothelial Cells

To further investigate the effect of miR-92a-3p on retinal ECs function, mimic-92a-3p was transfected into the human retinal microvascular endothelial cells (HRMECs) and then evaluated for its effects on tube formation, cell migration, and wound healing. Compared with the mimic-NC, the expression level of miR-92a-3p in HRMECs was increased in the mimic-92a-3p group (Fig. 5A;  $P = 0.001$  to  $< 0.01$ ). Compared with the mimic-NC, the mimic-92a-3p significantly decreased the ability of cell migration (Figs. 5B, 5C;  $P < 0.0001$ ), tube formation (Figs. 5D–5F;  $P = 0.0019$  to  $< 0.01$ ,  $P =$

0.0003 to  $< 0.001$ ), and wound healing (Figs. 5G, H;  $P = 0.0161$  to  $< 0.05$ ) in HRMECs. Together, these results indicated that miR-92a-3p was a potent suppressor of angiogenesis that might cause impairment through vascular EC function.

### Analysis of the Potential Target Genes of miR-92a-3p

To identify potential target genes of miR-92a-3p, we performed bioinformatics (Supplementary Materials and Methods) and high-throughput sequencing (Fig. 6A) analysis. First, a total of 699 common target genes were found (Supplementary Fig. S2). Next, the top 20 Gene Ontology (GO) and Kyoto Encyclopedia of Genes and Genomes (KEGG) items of the 699 genes were significantly enriched (Supplementary Fig. S3). The significantly enriched items for GO biological processes (BPs) were transcription, DNA-templated, positive regulation of transcription from the RNA polymerase II promoter, negative regulation of transcription from the RNA polymerase II promoter, intracellular signal transduction, and cell migration (see Supplementary Fig. S3A). In addition, the nucleus, cytoplasm, nucleoplasm, and membrane accounted for the majority of terms of the GO cellular components (CCs; see Supplementary Fig. S3B). The most enriched GO molecular functions (MFs) were protein binding, transcription factor activity, sequence-specific DNA binding, protein serine/threonine kinase activity, and protein kinase binding (see Supplementary Fig. S3C). KEGG pathway enrichment analysis showed that 11 of the top 20 pathways were closely associated with angiogenesis (see Supplementary Fig. S3D black arrow). The 11 KEGG pathways and related 63 key genes were identified (Supplementary Table S3). Last, to further capture the relationships among the 63 key gene terms, a subset of enriched terms



was selected and rendered as a network plot. We selected the terms with the best  $P$  values from each of the 20 clusters and visualized them using Cytoscape,<sup>20</sup> with each node representing an enriched term and colored first by its cluster ID (Supplementary Fig. S4A). Protein interaction enrichment analysis was applied to each Molecular Complex Detection (MCODE) component independently (see Supplementary Fig. S4B), and the three best-scoring terms by  $P$  values were retained as the functional description of the corresponding components (Supplementary Table S4). Using the genes in the Regulation of Actin Cytoskeleton and the PI3K-Akt signaling pathway in combination with other

studies,<sup>17,21</sup> three candidates were identified as associated with angiogenesis: ITGA5, PTEN, and SGK3. Additional miR-92a-3p targets include TMEM225B, NPIPA2, SULT1A4, LRRC24, CDRT4, U2AF1L5, C15orf38-AP3S2, and TMEM110-MUSTN1, predicted by high-throughput sequencing (see Fig. 6A).

### MiR-92a-3p Inhibits the Signal Pathway of SGK3 In Vivo and In Vitro

We analyzed the seed sequence of miR-92a-3p (CACGU-UAU), conserved in both human (see Fig. 6B) and mouse

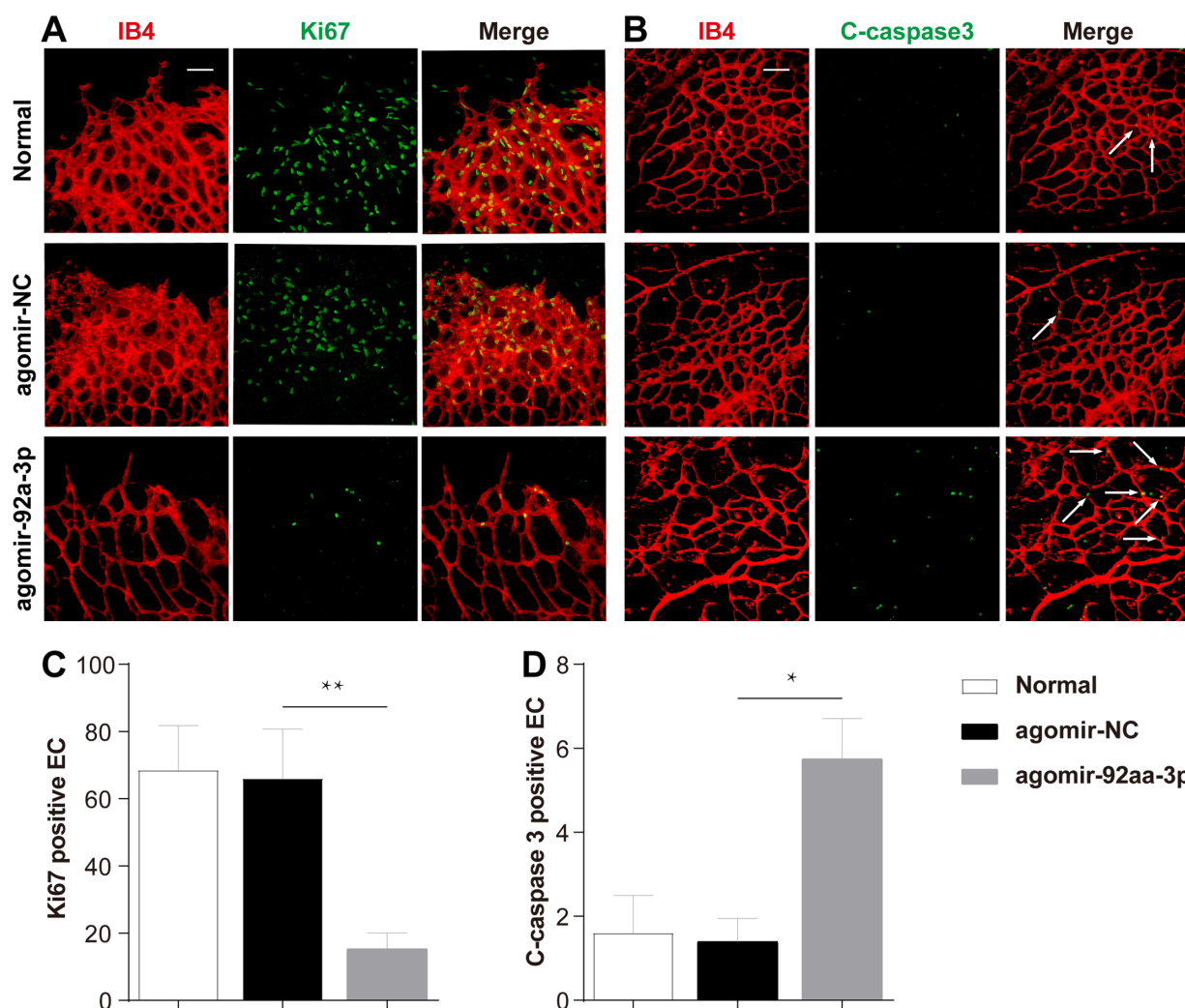


**FIGURE 4.** MiR-92a-3p alters proliferation and apoptosis of retinal vascular ECs. (A) Representative images of P7 mouse retinas injected with agomir-92a-3p or agomir-NC at P3, respectively, followed by staining with vascular marker IB4 (red) and the proliferation marker Ki67 (green) to observe the proliferation at the vascular front (scale bar = 100  $\mu$ m). (B) Representative images of P7 mouse retinas injected with agomir-92a-3p or agomir-NC at P3, respectively, followed by staining with IB4 (red) and apoptosis marker cleaved-caspase3 (green, white arrows) to observe the apoptosis at the proximal retina (scale bar = 100  $\mu$ m). (C) Retinas treated with agomir-92a-3p exhibiting fewer ECs positive for Ki67. (D) Agomir-92a-3p groups stained with cleaved-caspase3 revealing a significant increase in the proximal retina compared to the agomir-NC and normal groups. The data are presented as mean  $\pm$  SD ( $n$  = approximately 3–6 per group). \* $P$  < 0.05, \*\* $P$  < 0.01.

(Fig. 7A), for complementarity with SGK3. The mRNA levels of SGK3 in HRMECs treated with mimic-92a-3p (see Fig. 6C;  $P$  = 0.0049 to <0.01) and in P3 mouse retina intravitreally injected with agomir-92a-3p (see Fig. 7B;  $P$  = 0.0152 to <0.05) were markedly reduced at P7 compared with the NC group. Moreover, overexpression of miR-92a-3p in HRMECs (see Figs. 6D, 6E) and mouse retina (see Figs. 7C, 7E) significantly reduced the protein expression of SGK3, p-GSK3 $\beta$ /GSK3 $\beta$ , and Bcl-xL ( $P$  < 0.05). However, the cleaved caspase-3 increased in P7 mouse retinas (Figs. 7D, 7E [right];  $P$  < 0.05). Our findings suggest that miR-92a-3p affects the functions of HRMECs and retinal angiogenesis by directly inhibiting SGK3, then reduces the phosphorylation of GSK3 $\beta$ , and finally affects the formation of blood vessels. On the other hand, SGK3 also reduces the level of anti-apoptotic genes Bcl-xL and increases apoptotic genes cleaved caspase-3 before affecting the survival of vascular ECs and then inhibiting retinal angiogenesis.

### MiR-92a-3p Inhibits Retinal Neovascularization in the Oxygen-Induced Retinopathy Mouse Model

To determine whether miR-92a-3p contributes to regulating pathological angiogenesis, the oxygen-induced retinopathy (OIR) mice were established (Supplementary Fig. S5). The right eyes of OIR mice were treated with intravitreal injection of agomir-92a-3p at P12, whereas the left eyes have been intravitreally injected with agomir-NC. The OIR mice have been analyzed at P17 for the expression level of miR-92a-3p in their retinas. As expected, the right retinas treated with agomir-92a-3p showed an increased expression of miR-92a-3p compared to the left retinas treated with the agomir-NC (Fig. 8A;  $P$  = 0.0333 to <0.05). At P17, miR-92a-3p significantly suppressed retinal neovascularization in the right eyes of OIR mice compared with their left eyes injected with agomir-NC (Figs. 8B, 8C;  $P$  = 0.0257 to <0.05). Moreover, the expression levels of

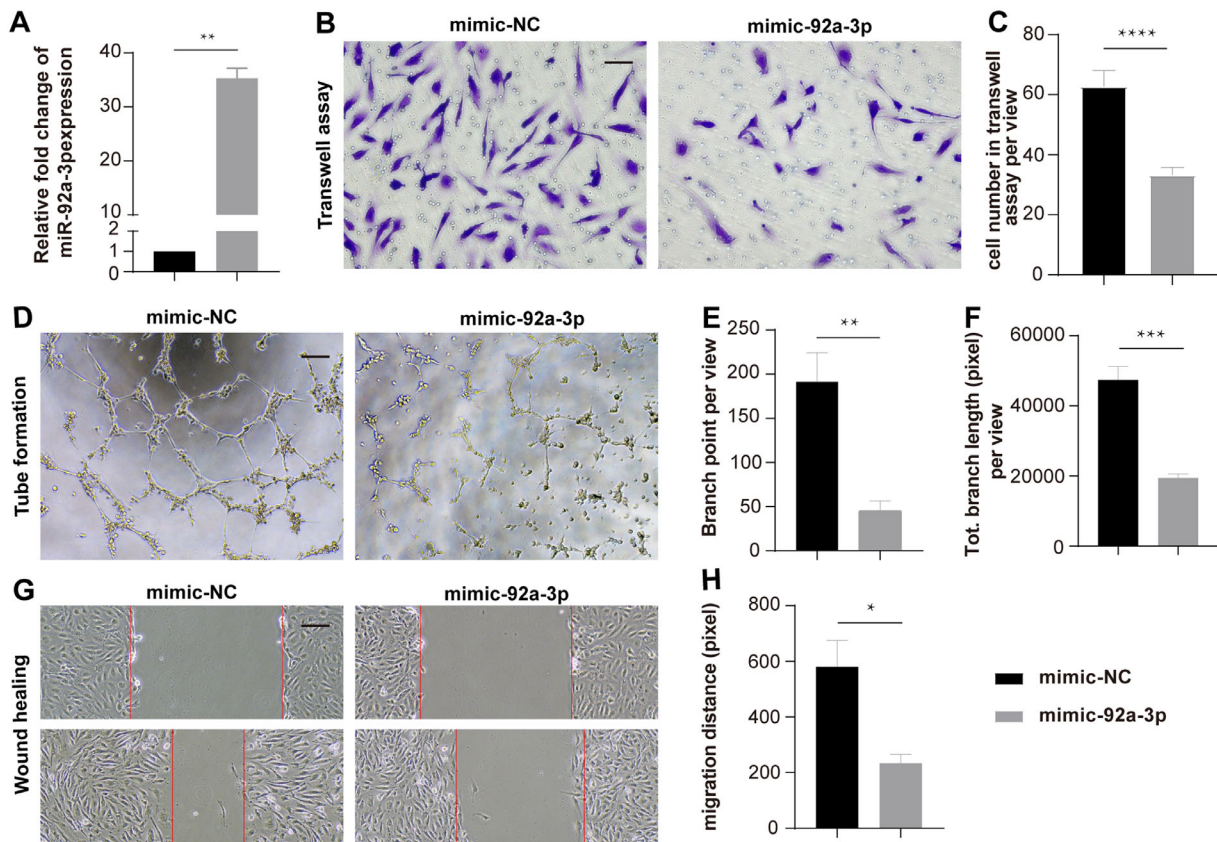


**FIGURE 5.** MiR-92a-3p suppresses the tube formation, proliferation, and migration of HRMECs in vitro. (A) Relative miR-92a-3p expression level in the HRMECs treated with mimic-92a-3p or mimic-NC. (B) Representative images of transwell assay in the HRMECs transfected with mimic-92a-3p or mimic-NC (scale bar = 50  $\mu$ m). (C) Quantitative analysis of cell numbers in the HRMECs transwell assay, showing a significant decrease in the mimic-92a-3p group compared to the mimic-NC group. (D) Representative images of tube formation assay in the HRMECs transfected with mimic-92a-3p or mimic-NC (100  $\mu$ m). (E, F) Quantitative analysis of the branch points and total branch length in the HRMECs tube formation, showing a significant decrease in the mimic-92a-3p group compared to the mimic-NC group. (G) Representative images of the HRMECs wound healing assay in the mimic-92a-3p or mimic-NC group (100  $\mu$ m). (H) Quantitative analysis of the migration distance in the HRMECs wound healing, showing a significant decrease in the mimic-92a-3p group compared to the mimic-NC group. The data are presented as means  $\pm$  SD ( $n = 3$  per group). \* $P < 0.05$ , \*\* $P < 0.01$ , \*\*\* $P < 0.001$ , \*\*\*\* $P < 0.0001$ .

SGK3, p-GSK3 $\beta$ /GSK3 $\beta$ , and Bcl-xL were also significantly decreased in agomir-92a-3p-treated P17 OIR retinas (see Figs. 8D, 8E;  $P < 0.05$ ). Together, these data suggest that miR-92a-3p suppressed pathological retinal neovascularization in OIR mice by targeting SGK3, p-GSK3 $\beta$ /GSK3 $\beta$ , and Bcl-xL.

## DISCUSSION

In the postnatal eye development mouse model, which is an ideal tool to visualize retinal vascular development, the retinal vessels start from the optic nerve after birth and form a superficial vascular plexus to the peripheral parts until P8 days<sup>22</sup>; the deep vascular plexus in the posterior pole are driving from the superficial retinal layer at P7 and extend to the peripheral part at P12.<sup>23</sup> Our study indicates that the overall expression of miR-92a-3p gradually decreases and is higher during the development of superficial retinal vessels (P0–P7) than in the development of deep retinal vessels (P8–P17). It is reasonable to speculate that miR-92a-3p might play an important role in retinal vascular development. Together with miR-17, -18a, -19a/b, -20a, and miR-92a, miR-92a

is a member of the miR-17-92 cluster, which is the first tumor-related miRNA found in lymphoma.<sup>24</sup> MiR-92a can promote the proliferation of lung cancer<sup>25</sup> and regulate the growth, development, and differentiation of the hematopoietic immune and cardiopulmonary system.<sup>26,27</sup> The miR-17-92 cluster is also found to be enriched in ECs.<sup>28,29</sup> Overexpression of the miR-17-92 cluster can promote tumor angiogenesis.<sup>16</sup> We hypothesized that miR-92a-3p might be involved in the initiation and progression of retinal vascular development. Although the miR-17-92 cluster is implicated in the development of tumor angiogenesis,<sup>30</sup> few studies have focused on retinal angiogenesis. To our knowledge, this is the first research to investigate the effect and mechanism of miR-92a-3p on retinal angiogenesis. In our study, intravitreal injection of agomir-92a-3p on P3, P5, and P9, respectively, delayed vascular development in both the superficial and deep retinal plexus. The overexpression of miR-92a-3p showed an anti-angiogenic effect that included decreases in the vessel density and the number of tip cells in the superficial retinal vessels at P7, as well as the suppression of intraretinal vessels diving from the superficial layer in the posterior retina at P9, and peripheral retina at P12 during retinal development. However, the overexpression of

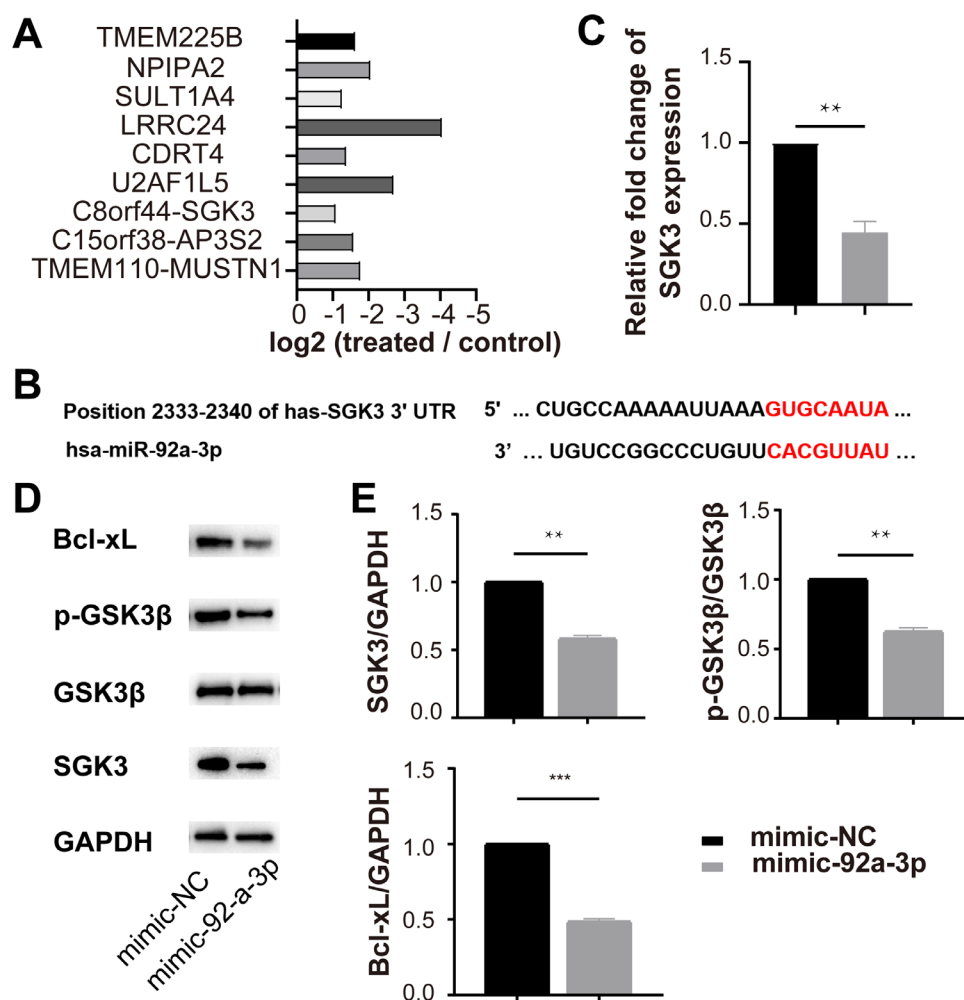


**FIGURE 6.** MiR-92a-3p overexpression suppressed angiogenesis by targeting SGK3 in vitro-cultured ECs. (A) Results of the high-throughput sequencing of differentially expressed genes after mimic-92a-3p transfection compared to that of mimic-NC. (B) Alignment between the binding sites of has-miR-92a-3p and SGK3. (C) The expression level of SGK3 mRNA was significantly down-regulated in the mimic-92a-3p group compared to the mimic-NC group. (D, E) Western blot analyses showing significant suppression of protein expression in SGK3, p-GSK3β/GSK3β, and Bcl-xL by the mimic-92a-3p treatment. The data are presented as mean ± SD ( $n = 3$  per group). \*\* $P < 0.01$ , \*\*\* $P < 0.001$ .

miR-92a-3p showed no significant difference between the two groups in the posterior retina at P12, when the deep layer vessels had formed in the posterior retina at P9. Additionally, we found that miR-92a-3p suppressed pathological neovascularization in OIR mouse. These results suggest that, although miR-92a-3p is critical for the initiation and progression of physiological and pathological angiogenesis, it has little effect on normal retinal vessels that have already formed.

In addition to the *in vivo* mouse model used to demonstrate the functional role of miR-92a-3p in the developmental angiogenesis, we revealed that overexpression of miR-92a-3p inhibited the physiological angiogenesis of HRMECs *in vitro*. Our study showed that miR-92a-3p might be a potential intrinsic anti-angiogenic factor, consistent with previous research.<sup>31</sup> MiR-92a is highly expressed in many tumor tissues, such as colon cancer,<sup>32</sup> gastric cancer,<sup>33</sup> and pancreatic cancer,<sup>34</sup> promoting the proliferation, metastasis, and angiogenesis of tumor tissues. It is also enriched in human vascular ECs,<sup>35</sup> especially in the cardiovascu-

lar system.<sup>36</sup> The role of miR-92a in regulating angiogenesis is still considered to be controversial and may vary depending on the different experimental models. A recent study<sup>18</sup> shows that miR-92a-3p promotes angiogenesis in retinoblastoma. However, another study<sup>15</sup> shows the down-regulation of miR-92a improves angiogenesis both *in vitro* and *in vivo*. Interestingly, Zhang et al.<sup>14</sup> indicate that both up- and downregulation of miR-92a in the cultured human umbilical vein endothelial cells (HUVECs) could have pro-angiogenic effects under oxidative stress. Therefore, miR-92a-3p may play different roles under different conditions or in different diseases. In addition, the overexpression of the miR-17-92 cluster can inhibit the angiogenesis of ECs,<sup>30</sup> a finding similar to that of our study. Vascular ECs play an important role in angiogenesis.<sup>37-39</sup> Daniel et al. have reported that high expression of miR-92a inhibits the proliferation of VEGF-treated ECs.<sup>40</sup> We also found that miR-92a-3p inhibited the proliferation of ECs at the vascular front and enhanced the apoptosis of ECs at the proximal retina.



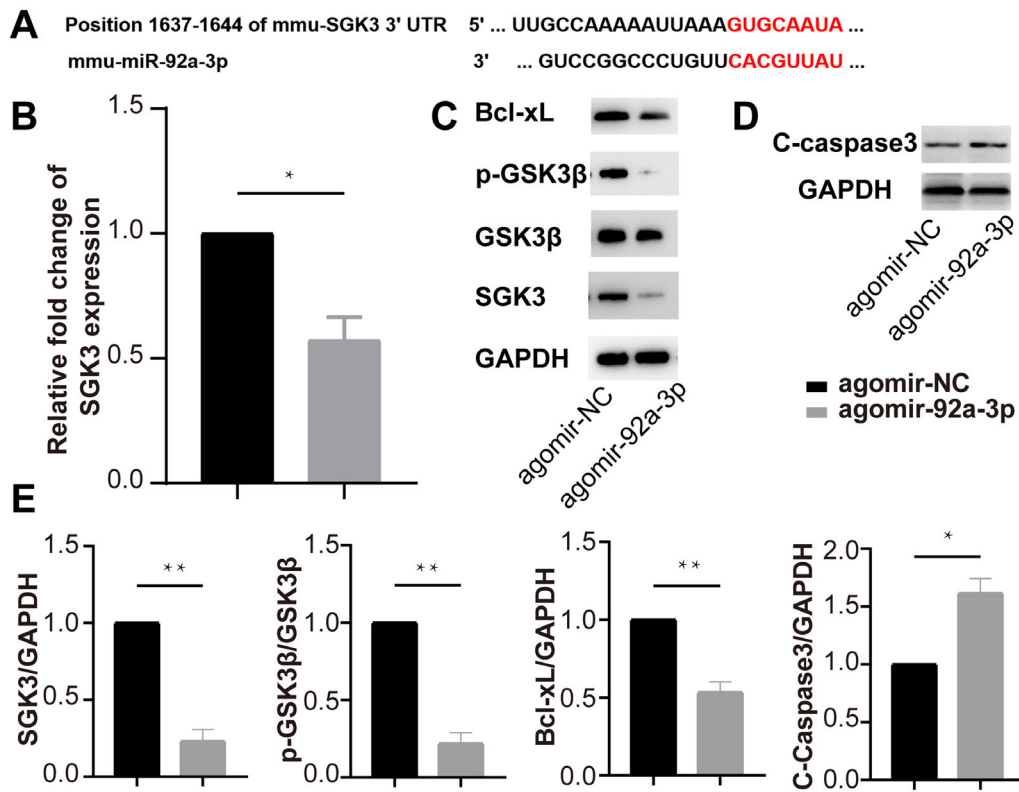


**FIGURE 7.** MiR-92a-3p overexpression suppresses retinal angiogenesis by targeting SGK3 in vivo. (A) Alignment between the binding sites of mmu-miR-92a-3p and SGK3. (B) Significant downregulation of the mRNA level of SGK3 in the agomir-92p-3p group compared to the agomir-NC group. (C, E [left 3]) Significant decrease in the protein levels of SGK3, p-GSK3β/GSK3β, and Bcl-xL in the agomir-92a-3p group. (D, E [right]) Agomir-92a-3p treatment significantly promoted the protein expression of cleaved-caspase3. The data are presented as mean ± SD (*n* = 3 per group). \**P* < 0.05, \*\**P* < 0.01.

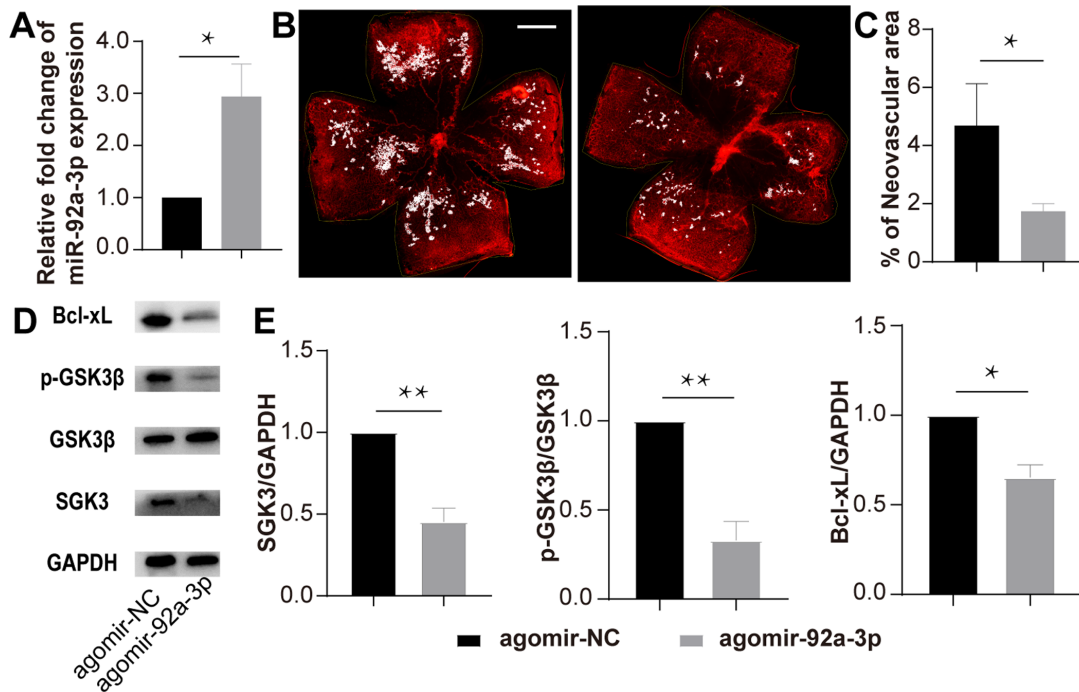


**FIGURE 8.** MiR-92a-3p inhibits retinal neovascularization by targeting SGK3 in OIR mouse. (A) The expression level of miR-92a-3p in OIR mouse treated with agomir-92a-3p was increased compared with agomir-NC group at P17. (B) Representative images of P17 mouse retinas injected with agomir-92a-3p or agomir-NC at P12, respectively, followed by staining with vascular marker IB4 to observe the neovascularization. Pathologic neovascular were labeled (*white highlight*). Scale bar = 200 μm. (C) Quantification of retinal neovascularization at P17 in OIR mice, showing that agomir-92a-3p treatment significantly reduced neovascularization in OIR retinas compared with the agomir-NC groups. (D, E) Western blot showing a significant suppression of protein expression in SGK3, p-GSK3β/GSK3β, and Bcl-xL by agomir-92a-3p treatment. The data are presented as mean ± SD (*n* = approximately 3–6 per group). \**P* < 0.05, \*\**P* < 0.01.

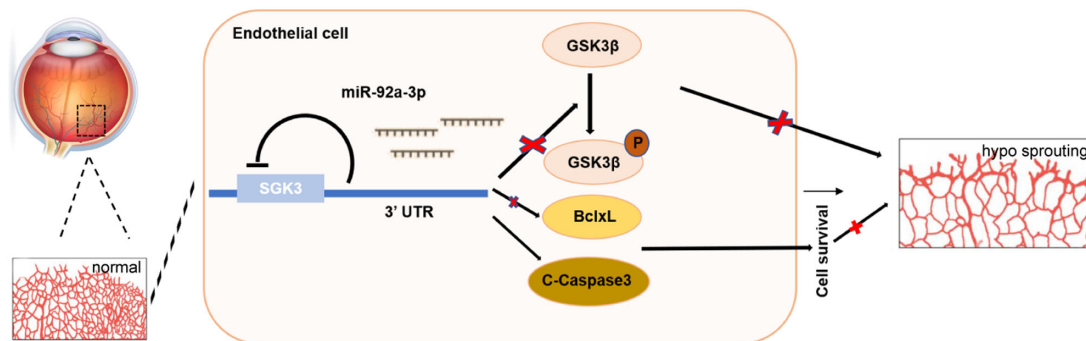


**FIGURE 9.** Proposed role of the miR-92a-3p-SGK3 axis in retinal angiogenesis. MiR-92a-3p affects retinal physiological and pathological angiogenesis by inhibiting the expression of SGK3 in retinal ECs, which suppresses the phosphorylation of GSK3 $\beta$ , decreases the expression of anti-apoptosis gene Bcl-xL, increases apoptosis gene cleaved caspase-3, and promotes the apoptosis of retinal vascular ECs.

Angiogenesis is a complex process that involves various events and signaling pathways. Gathered from three key prediction databases, the two predictively most enriched signaling pathways targeted by miR-92a-3p, namely FoxO pathway and focal adhesion, are indicative of a clearer role for miR-92a-3p in tip cell formation, vascular sprout formation, tubulogenesis, and vascular remodeling. Moreover, there have been numerous known target genes of miR-92a in regulating angiogenesis, such as KLF2, KLF4, and ITGA5,<sup>13,41,42</sup> which are mainly involved in the enriched signaling pathways. Novel targets of miR-92a are still under investigation. Interestingly, we found SGK3 was present in the top-scoring associated angiogenesis signaling pathway, computed from three databases of predicted miR-92a-3p target genes. SGK3 is an important member of the SGK family, which also includes SGK1 and SGK2. As a member of the AGC family, SGK3 is homologous with Akt in sequence<sup>43,44</sup>; they are thus also similar in function. SGK3 controls the processes of cell growth, proliferation, metabolism, and intracellular material exchange.<sup>45</sup> It has been reported that SGK3 may play an important role in tumor angiogenesis through the PI3K/Akt pathway, but there are still few studies on SGK3 and angiogenesis. Recently, some studies have described a relationship between GSK3 $\beta$  and angiogenesis.<sup>46–48</sup> GSK3 $\beta$  acts downstream of SGK3, and its phosphorylation can regulate angiogenesis. On the other hand, SGK3 can increase the level of Bcl-xL and inhibit the expression of the proapoptotic gene Bad.<sup>21,49</sup> Most importantly, in the present study, the overexpression of miR-92a-3p in P7 normal and P17 OIR mouse retinas, and HRMECs significantly reduced the mRNA and protein levels of SGK3. Comparison and analysis indicate that the seed sequence of miR-92a-3p is complementary to the sequence of SGK3. In addition, we also confirmed that SGK3 may be a direct target of miR-92a-3p in humans and mice. In line with the confirmation of SGK3 as miR-92a-3p target genes, the protein levels of p-GSK3 $\beta$ /GSK3 $\beta$  and Bcl-xL associated with SGK3 were also lower in the overexpression of miR-92a-3p groups in our study. Therefore, our results demonstrated that miR-92a-3p affected retinal angiogenesis by inhibiting the expression of SGK3 in retinal ECs, which suppressed the phosphorylation of GSK3 $\beta$ , decreased the expression of anti-apoptosis gene Bcl-xL, increased apoptosis gene cleaved caspase-3, and promoted the apoptosis of retinal vascular ECs (Fig. 9). Overall, this is the first study to demonstrate the essential role of miR-92a-3p in both regulating in vitro and in vivo

angiogenesis, especially in physiological and pathological retinal angiogenesis. This study presents evidence of miR-92a-3p as a regulator of vascular ECs angiogenesis in the development of mouse retinas. These findings provide new insight into targeting miR-92a-3p and the SGK3/GSK3 $\beta$  axis as a promising therapeutic way for retinal neovascularization diseases.

### Acknowledgments

Funded by the Natural Science Foundation of Guangdong Province to Y.L. (2020A1515010617), the National Natural Science Foundation of China to Y.L. (81770971), and the National Natural Science Foundation of China to Y.L. (81371020).

Disclosure: **Y. Cui**, None; **R. Liu**, None; **Y. Hong**, None; **Y. Wang**, None; **Y. Zhu**, None; **T. Wen**, None; **J. Lu**, None; **S. Mao**, None; **X. Wang**, None; **J. Pan**, None; **Y. Luo**, None

### References

- Kim SJ, Port AD, Swan R, Campbell JP, Chan RVP, Chiang MF. Retinopathy of prematurity: a review of risk factors and their clinical significance. *Surv Ophthalmol.* 2018;63(5):618–637.
- Song P, Xu Y, Zha M, Zhang Y, Rudan I. Global epidemiology of retinal vein occlusion: a systematic review and meta-analysis of prevalence, incidence, and risk factors. *J Glob Health.* 2019;9(1):010427.
- Yau JW, Rogers SL, Kawasaki R, et al. Global prevalence and major risk factors of diabetic retinopathy. *Diabetes Care.* 2012;35(3):556–564.
- Scott IU, VanVeldhuisen PC, Ip MS, et al. Effect of Bevacizumab vs Aflibercept on Visual Acuity Among Patients With Macular Edema Due to Central Retinal Vein Occlusion: The SCORE2 Randomized Clinical Trial. *Jama.* 2017;317(20):2072–2087.
- Campochiaro PA, Sophie R, Pearlman J, et al. Long-term outcomes in patients with retinal vein occlusion treated with ranibizumab: the RETAIN study. *Ophthalmology.* 2014;121(1):209–219.
- Lewis BP, Burge CB, Bartel DP. Conserved seed pairing, often flanked by adenosines, indicates that thousands of human genes are microRNA targets. *Cell.* 2005;120(1):15–20.
- Bartel DP. MicroRNAs: genomics, biogenesis, mechanism, and function. *Cell.* 2004;116(2):281–297.

8. La Torre A, Georgi S, Reh TA. Conserved microRNA pathway regulates developmental timing of retinal neurogenesis. *Proc Natl Acad Sci USA*. 2013;110(26):E2362–E2370.
9. Wang Y, Wang X, Jiang Y, et al. Identification of key miRNAs and genes for mouse retinal development using a linear model. *Mol Med Rep*. 2020;22(1):494–506.
10. Sun LL, Li WD, Lei FR, Li XQ. The regulatory role of microRNAs in angiogenesis-related diseases. *J Cell Mol Med*. 2018;22(10):4568–4587.
11. Hinkel R, Penzkofer D, Zühlke S, et al. Inhibition of microRNA-92a protects against ischemia/reperfusion injury in a large-animal model. *Circulation*. 2013;128(10):1066–1075.
12. Doebele C, Bonauer A, Fischer A, et al. Members of the microRNA-17-92 cluster exhibit a cell-intrinsic antiangiogenic function in endothelial cells. *Blood*. 2010;115(23):4944–4950.
13. Bonauer A, Carmona G, Iwasaki M, et al. MicroRNA-92a controls angiogenesis and functional recovery of ischemic tissues in mice. *Science*. 2009;324(5935):1710–1713.
14. Zhang L, Zhou M, Qin G, Weintraub NL, Tang Y. MiR-92a regulates viability and angiogenesis of endothelial cells under oxidative stress. *Biochem Biophys Res Commun*. 2014;446(4):952–958.
15. Radmanesh F, Sadeghi Abandansari H, Ghanian MH, et al. Hydrogel-mediated delivery of microRNA-92a inhibitor polyplex nanoparticles induces localized angiogenesis. *Angiogenesis*. 2021;24(3):657–676.
16. Dews M, Homayouni A, Yu D, et al. Augmentation of tumor angiogenesis by a Myc-activated microRNA cluster. *Nat Genet*. 2006;38(9):1060–1065.
17. Chamorro-Jorganes A, Lee MY, Araldi E, et al. VEGF-Induced Expression of miR-17-92 Cluster in Endothelial Cells Is Mediated by ERK/ELK1 Activation and Regulates Angiogenesis. *Circ Res*. 2016;118(1):38–47.
18. Chen S, Chen X, Luo Q, et al. Retinoblastoma cell-derived exosomes promote angiogenesis of human vesicle endothelial cells through microRNA-92a-3p. *Cell Death Dis*. 2021;12(7):695.
19. Benton RL, Maddie MA, Minnillo DR, Hagg T, Whittemore SR. Griffonia simplicifolia isolectin B4 identifies a specific subpopulation of angiogenic blood vessels following contusive spinal cord injury in the adult mouse. *J Comp Neurol*. 2008;507(1):1031–1052.
20. Shannon P, Markiel A, Ozier O, et al. Cytoscape: a software environment for integrated models of biomolecular interaction networks. *Genome Res*. 2003;13(11):2498–2504.
21. Bruhn MA, Pearson RB, Hannan RD, Sheppard KE. AKT-independent PI3-K signaling in cancer - emerging role for SGK3. *Cancer Manag Res*. 2013;5281–5292.
22. Fruttiger M. Development of the retinal vasculature. *Angiogenesis*. 2007;10(2):77–88.
23. Stahl A, Connor KM, Sapiha P, et al. The mouse retina as an angiogenesis model. *Invest Ophthalmol Vis Sci*. 2010;51(6):2813–2826.
24. He L, Thomson JM, Hemann MT, et al. A microRNA polycistron as a potential human oncogene. *Nature*. 2005;435(7043):828–833.
25. Hayashita Y, Osada H, Tatematsu Y, et al. A polycistronic microRNA cluster, miR-17-92, is overexpressed in human lung cancers and enhances cell proliferation. *Cancer Res*. 2005;65(21):9628–9632.
26. Koralov SB, Muljo SA, Galler GR, et al. Dicer ablation affects antibody diversity and cell survival in the B lymphocyte lineage. *Cell*. 2008;132(5):860–874.
27. Mogilyansky E, Rigoutsos I. The miR-17/92 cluster: a comprehensive update on its genomics, genetics, functions and increasingly important and numerous roles in health and disease. *Cell Death Differ*. 2013;20(12):1603–1614.
28. Kuehbachner A, Urbich C, Zeiher AM, Dimmeler S. Role of Dicer and Drosha for endothelial microRNA expression and angiogenesis. *Circ Res*. 2007;101(1):59–68.
29. Suárez Y, Fernández-Hernando C, Yu J, et al. Dicer-dependent endothelial microRNAs are necessary for post-natal angiogenesis. *Proc Natl Acad Sci USA*. 2008;105(37):14082–14087.
30. Esquela-Kerscher A, Slack FJ. Oncomirs - microRNAs with a role in cancer. *Nat Rev Cancer*. 2006;6(4):259–269.
31. Li S, Yuan L, Su L, et al. Decreased miR-92a-3p expression potentially mediates the pro-angiogenic effects of oxidative stress-activated endothelial cell-derived exosomes by targeting tissue factor. *Int J Mol Med*. 2020;46(5):1886–1898.
32. Tsuchida A, Ohno S, Wu W, et al. miR-92 is a key oncogenic component of the miR-17-92 cluster in colon cancer. *Cancer Sci*. 2011;102(12):2264–2271.
33. Fan B, Shen C, Wu M, Zhao J, Guo Q, Luo Y. miR-17-92 cluster is connected with disease progression and oxaliplatin/capecitabine chemotherapy efficacy in advanced gastric cancer patients: A preliminary study. *Medicine (Baltimore)*. 2018;97(35):e12007.
34. He G, Zhang L, Li Q, Yang L. miR-92a/DUSP10/JNK signalling axis promotes human pancreatic cancer cells proliferation. *Biomed Pharmacother*. 2014;68(1):25–30.
35. Liu H, Wu HY, Wang WY, Zhao ZL, Liu XY, Wang LY. Regulation of miR-92a on vascular endothelial aging via mediating Nrf2-KEAP1-ARE signal pathway. *Eur Rev Med Pharmacol Sci*. 2017;21(11):2734–2742.
36. Liu H, Li G, Zhao W, Hu Y. Inhibition of MiR-92a May Protect Endothelial Cells After Acute Myocardial Infarction in Rats: Role of KLF2/4. *Med Sci Monit*. 2016;22:2451–2462.
37. Zhu S, Bennett S, Kuek V, et al. Endothelial cells produce angiocrine factors to regulate bone and cartilage via versatile mechanisms. *Theranostics*. 2020;10(13):5957–5965.
38. Selvam S, Kumar T, Fruttiger M. Retinal vasculature development in health and disease. *Prog Retin Eye Res*. 2018;63:1–19.
39. Lee MY, Luciano AK, Ackah E, et al. Endothelial Akt1 mediates angiogenesis by phosphorylating multiple angiogenic substrates. *Proc Natl Acad Sci USA*. 2014;111(35):12865–12870.
40. Daniel JM, Penzkofer D, Teske R, et al. Inhibition of miR-92a improves re-endothelialization and prevents neointima formation following vascular injury. *Cardiovasc Res*. 2014;103(4):564–572.
41. Shyu KG, Wang BW, Pan CM, Fang WJ, Lin CM. Hyperbaric oxygen boosts long noncoding RNA MALAT1 exosome secretion to suppress microRNA-92a expression in therapeutic angiogenesis. *Int J Cardiol*. 2019;274:271–278.
42. Iaconetti C, Polimeni A, Sorrentino S, et al. Inhibition of miR-92a increases endothelial proliferation and migration in vitro as well as reduces neointimal proliferation in vivo after vascular injury. *Basic Res Cardiol*. 2012;107(5):296.
43. Xu J, Liu D, Gill G, Songyang Z. Regulation of cytokine-independent survival kinase (CISK) by the Phox homology domain and phosphoinositides. *J Cell Biol*. 2001;154(4):699–705.
44. Xu J, Wan M, He Q, et al. SGK3 is associated with estrogen receptor expression in breast cancer. *Breast Cancer Res Treat*. 2012;134(2):531–541.
45. Pearce LR, Komander D, Alessi DR. The nuts and bolts of AGC protein kinases. *Nat Rev Mol Cell Biol*. 2010;11(1):9–22.
46. Zhang Y, Cheng H, Li W, Wu H, Yang Y. Highly-expressed P2X7 receptor promotes growth and metastasis of human HOS/MNNG osteosarcoma cells via PI3K/Akt/GSK3 $\beta$ / $\beta$ -

- catenin and mTOR/HIF1 $\alpha$ /VEGF signaling. *Int J Cancer*. 2019;145(4):1068–1082.
47. Dai J, Wei R, Zhang P, Kong B. Overexpression of microRNA-195-5p reduces cisplatin resistance and angiogenesis in ovarian cancer by inhibiting the PSAT1-dependent GSK3 $\beta$ / $\beta$ -catenin signaling pathway. *J Transl Med*. 2019;17(1):190.
  48. Li R, Liu Z, Wu X, Yu Z, Zhao S, Tang X. Lithium chloride promoted hematoma resolution after intracerebral hemorrhage through GSK-3 $\beta$ -mediated pathways-dependent microglia phagocytosis and M2-phenotype differentiation, angiogenesis and neurogenesis in a rat model. *Brain Res Bull*. 2019;152:117–127.
  49. Ellson CD, Andrews S, Stephens LR, Hawkins PT. The PX domain: a new phosphoinositide-binding module. *J Cell Sci*. 2002;115(Pt 6):1099–1105.
  50. Luo Y, Xiao W, Zhu X, et al. Differential expression of claudins in retinas during normal development and the angiogenesis of oxygen-induced retinopathy. *Invest Ophthalmol Vis Sci*. 2011;52(10):7556–7564.
  51. Chen J, Connor KM, Aderman CM, Willett KL, Aspegren OP, Smith LE. Suppression of retinal neovascularization by erythropoietin siRNA in a mouse model of proliferative retinopathy. *Invest Ophthalmol Vis Sci*. 2009;50(3):1329–1335.
  52. Bai Y, Bai X, Wang Z, Zhang X, Ruan C, Miao J. MicroRNA-126 inhibits ischemia-induced retinal neovascularization via regulating angiogenic growth factors. *Exp Mol Pathol*. 2011;91(1):471–477.
  53. Stenvang J, Petri A, Lindow M, Obad S, Kauppinen S. Inhibition of microRNA function by anti-miR oligonucleotides. *Silence*. 2012;3(1):1.
  54. Cao D, Li J, Wang X, et al. The effect of AAV-mediated down-regulation of Claudin-3 on the development of mouse retinal vasculature. *Exp Eye Res*. 2021;213:108836.
  55. Langmead B, Salzberg SL. Fast gapped-read alignment with Bowtie 2. *Nat Methods*. 2012;9(4):357–359.
  56. Li B, Dewey CN. RSEM: accurate transcript quantification from RNA-Seq data with or without a reference genome. *BMC Bioinformatics*. 2011;12:323.
  57. Wang L, Feng Z, Wang X, Wang X, Zhang X. DEGseq: an R package for identifying differentially expressed genes from RNA-seq data. *Bioinformatics*. 2010;26(1):136–138.